

Imaging of the Muscle-Bone Relationship

Alex Ireland · José Luis Ferretti · Jörn Rittweger

© Springer Science+Business Media New York 2014

Abstract Muscle can be assessed by imaging techniques according to its size (as thickness, area, volume, or alternatively, as a mass) and architecture (fiber length and pennation angle), with values used as an anthropometric measure or a surrogate for force production. Similarly, the size of the bone (as area or volume) can be imaged using MRI or pQCT, although typically bone mineral mass is reported. Bone imaging measures of mineral density, size, and geometry can also be combined to calculate bone's structural strength—measures being highly predictive of bone's failure load *ex vivo*. Imaging of muscle-bone relationships can, hence, be accomplished through a number of approaches by adoption and comparison of these different muscle and bone parameters, dependent on the research question under investigation. These approaches have revealed evidence of direct, mechanical muscle-bone interactions independent of allometric associations. They have led to important information on bone mechanoadaptation and the influence of muscular action on bone, in addition to influences of age, gender, exercise, and disuse on muscle-bone relationships. Such analyses have also produced promising diagnostic tools for clinical use, such as identification of primary, disuse-induced, and secondary osteoporosis and estimation of bone safety factors. Standardization of muscle-bone imaging methods is required to permit more reliable comparisons between studies and differing

imaging modes, and in particular to aid adoption of these methods into widespread clinical practice.

Keywords Muscle · Bone · Imaging · BMD · DEXA · pQCT

Imaging the Problem

The dynamic muscle-bone relationships can be analyzed by imaging masses, structures, and their interactions [1]. Imaging masses requires analysis of anthropometric features related to nondirectional magnitudes. Imaging structures involves analyses of direction-related properties. Imaging interactions requires the analysis of mathematical relationships between image-derived, directional, and nondirectional variables. There are 3 particularly attractive approaches to those purposes, namely, (1) imaging muscle mass and structure as force generators, and imaging bone mass/structure concerning their ability to (2) transform forces into stress and (3) adapt to stress (force/area values).

Imaging Muscles as Force-Generators

The power-generating step in muscle contractions is the cross-bridge interaction between myosin and actin filaments [2]. Force, and velocity, of a given contraction are, therefore, determined by the number of active cross-bridges. Within skeletal muscle fibers, actin, and myosin filaments are parallel-aligned and neatly bundled into sarcomeres, thus, endowing the many cross-bridges with a direction. Muscle force increases with the number of sarcomeres-in-parallel, whilst contraction velocity increases with the number of sarcomeres-in-series [3]. Therefore, as an anatomic approximation of a muscle's, or a muscle group's force generating capacity we can identify the cross-sectional area (CSA). The anatomic CSA (aCSA), ie, the CSA perpendicular to the

A. Ireland

Cognitive Motor Function Research Group, Manchester Metropolitan University, Manchester, England

J. L. Ferretti

Center of P-Ca Metabolism Studies (CEMFOC), Faculty of Medicine, National University of Rosario, Rosario, Argentina

J. Rittweger (✉)

Institute of Aerospace Medicine, German Aerospace Centre, Linder Höhe, 51147 Cologne, Germany
e-mail: j.rittweger@dlr.de

origin-insertion axis, is easily identifiable with conventional X-ray based or conventional T1 or T2-weighted magnetic resonance (MR) images. The physiological CSA (pCSA) takes into account the pennation angle in those muscles (Fig. 1), where the fibers' direction deviates from the anatomic axis of the muscle, which is the case for most of our muscles. Mathematically speaking, pennation packs more sarcomeres-in-parallel into a volume, albeit at the expense of reducing contraction speed. pCSA is a better predictor of a muscle's force generating capacity than aCSA [4]. To assess it requires measurement of the pennation angle, which can be done by ultrasound for parts of a muscle, or with MR diffusion tensor imaging [5].

Imaging Bone Ability to Receive Forces

At the tissue level, bone has properties of material stiffness (the degree of deformation under a given stress), material strength (ability to resist fracture), and toughness (ability to dissipate energy). The stiffness of cortical and trabecular bone as a material is strongly associated with bone mineral density [6, 7], which can be measured by cross-sectional densitometric techniques such as peripheral quantitative computed tomography (pQCT).

As an organ, a bone also has properties of structural stiffness and toughness, both of which together determine its strength (the maximal stress the bone can stand until fracture). There are 3 principle kinds of strains and stresses, namely compression, tension, and shear. Bones as structures can experience many different kinds of deformations, of which loading in bending and torsion are common examples. Strength/stiffness in compression is related to bone mass in the cross-section orthogonal to the applied stress. Assuming invariant density, a larger bone cross-section results in greater bone mineral content (BMC) - measures which are more strongly correlated with axial bone strength than BMD measures alone [8, 9]. Measurement of bone diameters, or periosteal and endocortical perimeters describe changes in bone shape or cortical thickness which can evaluate some relative or combined effects on the corresponding, periosteal and endocortical surfaces. However, the distribution of bone mass relative to the center of mass also affects its stiffness and strength in bending and torsion. Cross-sectional moment of inertia (CSMI) of the cortical bone area in long bones

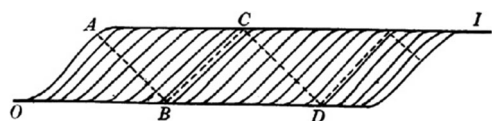


Fig. 1 Diagram of a unipennate muscle indicating fiber orientation (solid diagonal lines), line BC indicates appropriate plane for measurement of physiological cross-sectional area (pCSA). Anatomic cross-sectional area (aCSA) is that resulting from a section orthogonal to the upper aponeurosis line ACI. Reproduced with permission from [4]

indicates bone's stiffness in bending (axial CSMI) or torsion (polar CSMI) and is calculated as the sum of the voxel areas multiplied by the square of the distance (either in a single plane in the case of axial CSMI, or absolute distance in the case of polar CSMI) of each voxel from the center of bone mass (Fig. 2). Moment of resistance (alternatively known as section modulus) is calculated by dividing the moment of inertia by the outer radius and indicates bone's strength in bending or torsion. Therefore—for example—the same bone mass organized into a large diameter, thin-walled tube will be stiffer in torsion (and indeed in bending) than a small diameter, thick-walled tube.

The relationships between CSMI and bone strength tend to vanish when bone diameter is proportionally much larger than cortical thickness. In this situation, CSMI can be very large, but the bone can fail in buckling. The tendency to do so is estimated by the buckling ratio = periosteal diameter / cortical thickness. Within these limitations, the CSMI can be combined with tissue mineral density to create density-weighted moments of inertia (also known as Bone Strength Index BSI). BSI has been shown to be a stronger predictor of bone breaking strength than its components CSMI or cortical BMD, explaining 89 % of variance in strength [10]. Similarly, density-weighted section modulus (strength-strain index or SSI) has been derived, and explained 98 % of variance in fracture load in human tibia—this association being stronger than those between fracture load and other bone measures such as cortical area and section modulus without density weighting [11].

Imaging Bone Ability to Adapt to the Mechanical Environment

Within-Bone Relationships

Bone modeling and remodeling can be both modulated and spatially-oriented as a function of mechanical usage by bone

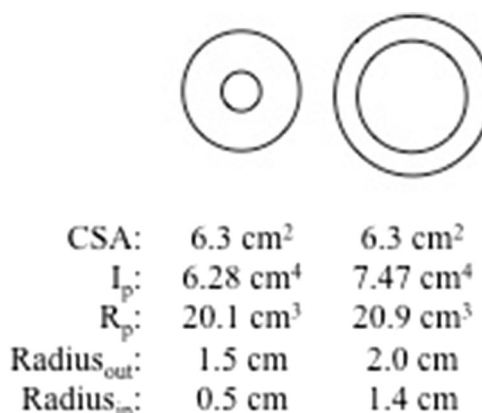


Fig. 2 Geometrical properties and strength in cylinders. CSA Cross-sectional area, I_p Polar moment of inertia, Radius_{in} inner cylinder radius, Radius_{out} outer cylinder radius, R_p Polar moment of resistance

mechanostat. This can result in re-orientation of cortical shells and trabecular networks as structural adaptations of bone tissue distribution to the induced stresses. These bone properties can be assessed by correlating different image-derived indicators of geometric properties (y) as a function of indicators of bone tissue mass (x_1), as “distribution/mass” (d/m) relationships, or stiffness (x_2), as “distribution/quality” (d/q) relationships (Fig. 3).

Muscle-Bone Associations and Interactions

These can be assessed by imaging 4 different kinds of general (ubiquitous) muscle/bone associations, namely, (1) mass/mass (anthropometric), (2) structure/force (mechanical, translational), (3) structure/structure (mechanical, static), and (4) force/stress (mechanical, dynamic) relationships, as well as (5) some site-specific applications of the same, as follows.

Overview of the Particular Matters Involved in the Analysis OF Muscle-Bone—Associations and Interactions

General Approaches

Imaging Muscle/Bone Mass/Mass (Anthropometric) Relationships

The biomechanical influences of muscles on bones as assessed by mass/mass relationships are blunted by natural morphogenetic associations [13–18], yet there is some evidence of a direct, mechanical interaction [19–23]. In fact, DXA studies of the whole-body and limbs (standard determinations of lumbar spine, femur, and radius are unsuitable for this purpose) have shown that mineral (BMC, y) and lean (related to muscle, x) masses are linearly related in both sexes at any age with similar slopes [24–29] (Fig. 4). However, the intercepts of those relationships differed in the order:

children < men = post-MP women < pre-MP women [30, 31]. While similar slopes are compatible with the identity of bone mechanostat in the species [32], different intercepts would indicate the agonistic interference of sex hormones in the mechanical control of bone features [33].

We have standardized those relationships for whole-body and limb measures in 3000+ normal men and women and provided Z-scored charts for comparative diagnoses of osteopenia [34] which are specific to the type of device employed (Fig. 5). Importantly, these relationships do not capture any structural variable related to actual muscle and bone strength [35]. However, the charts allow proposal of a predominantly “mechanical” or “metabolic” nature of the studied osteopenia (not osteoporosis) when compared with the values of BMC/lean mass ratio and lean mass data of the studied individual, respectively [36].

This distinction may orient the therapeutic indications of physical or pharmacologic treatments. Low bone/muscle proportionalities were observed in post-MP women with typically osteoporotic fractures [37]; in thyroparathyroidectomized children [38]; in very lean, amenorrheic female ballet dancers, and in chronically hemodialyzed patients [unpublished].

Imaging Muscle/Muscle Structure/Structure (Mechanical, Translational) Relationships (Combined Cross-Sectional (pQCT, etc) + Dynamometric Methodologies) → Muscle Analysis

As previously discussed, and *ceteris parabus*, a larger muscle will produce greater force. Imaging of muscle size by MRI has revealed strong associations between measures and maximal force. However, muscle size can be assessed as a 3-(volume), 2-(CSA) or 1-dimensional (thickness) scalar measure. Owing to time or equipment restrictions single site assessments of cross-sectional area or muscle thickness are commonly measured in lieu of muscle volume. The 3 values are unsurprisingly highly correlated [39] and are each also strongly related to maximal force [40–42]. Comparisons of the predictive ability of their different measures have produced varying

Fig. 3 Typical “distribution/mass” (d/m, left) and “distribution/quality” (d/q, right) curves obtained from scans taken at 40 % (d/m) and at 65 % (d/q) of the tibia height in male and female individuals who were untrained (S) or trained in long-distance running (R) [12•]

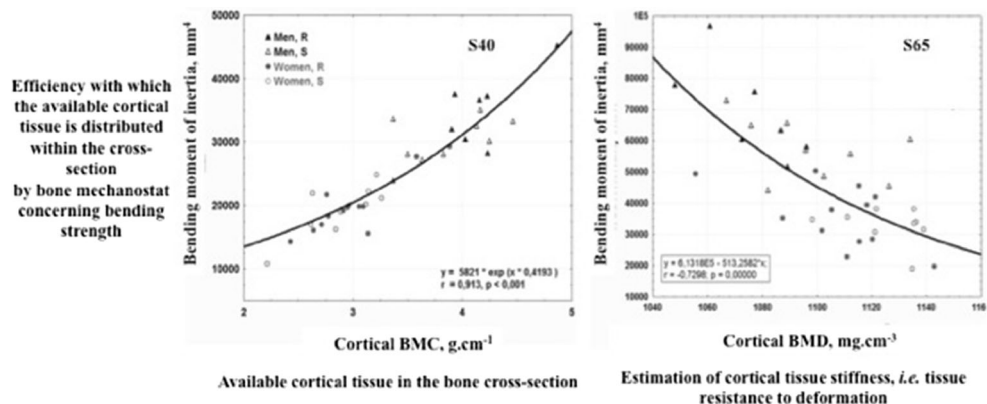
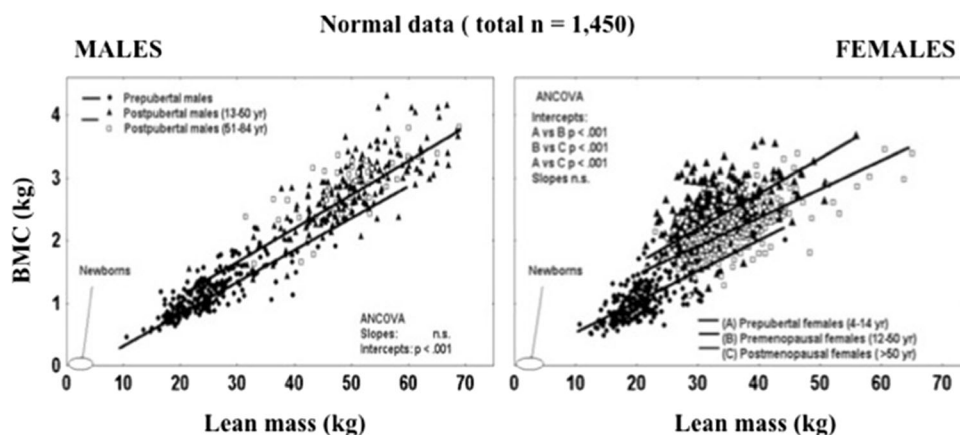


Fig. 4 Relationships between the DXA-assessed, whole-bone BMC (y) and lean mass(x) of a representative sample of healthy children, men, and pre- and postmenopausal women [30]



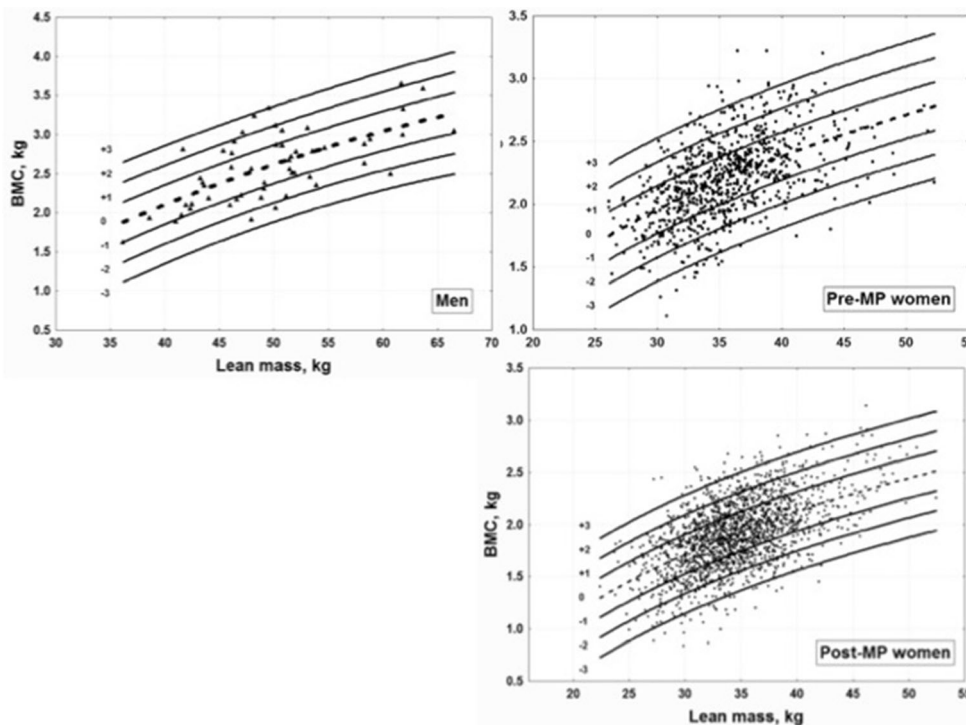
results, with MRI-assessed elbow extensor and flexor volume explaining over 90 % of variance in the isometric joint torques produced by their respective actions, whereas associations between torque and muscle CSA, and muscle thickness assessed by ultrasound in the same participants were weaker [42]. Conversely, other studies have shown similar relationships between maximal force and muscle CSA or volume [43].

Imaging muscle bone relationships makes the inherent assumption that all muscles have identical intrinsic strength, *ie*, generate the same peak tension. This is, of course, not generally true. Old age and immobilization-induced atrophy, for example, entail reductions in the peak tension of isolated muscle fibers [44]. The latter effect seems to be caused by reduced concentration of contractile apparatus within the

muscle cells. Moreover, muscle dystrophic disorders [45], multiple sclerosis [46], and possibly others. There is a long and undecided debate whether or not children have lower intrinsic strength than adults [47–49].

Boundaries such as age and clinical disorders must therefore be considered when using muscle CSA for clinical and scientific inferences. Attempts have been made to obtain detail of differences in size-adjusted force or ‘muscle quality’ by imaging methods. One such method is analysis of muscle X-ray attenuation (MXA) as obtained from computed tomography. MXA decreases with age [50] and is associated with specific tension of a muscle [51]. However, a lack of understanding of the physiological properties of muscle underlying MXA values is likely responsible for the lack of widespread adoption of the technique.

Fig. 5 Z-scored charts of the relationships between the DXA-assessed, whole-bone BMC (y) and lean mass (x) of a representative sample of healthy men and pre- and postmenopausal women [34]



Imaging Muscle/Bone Structure/Structure (Mechanical, Static) Relationships (Cross-Sectional Methodologies Only) → Bone Mass, Material Quality, Design and/or Strength Indicators vs Muscle Mass, Cross-Sectional Properties, and/or Force Indicators; Muscle-Bone Strength Indices) → Classification of Osteoporoses

Beyond the meaningfulness of anthropometric muscle-bone mass/mass relationships (previously mentioned), the biomechanical muscle-bone associations can be approached more specifically by comparing image analyses of bone features and muscle characteristics previously described. To this purpose, it is generally preferable to select cross-sectional imaging data, as provided by QCT, pQCT, or similar techniques, rather than “areal” DXA data. Many of the variables measured cross-sectionally can be regarded as indicators of bone mass (total, trabecular or cortical BMC, total or cortical bone area, total or trabecular vBMD), bone material stiffness (cortical vBMD), bone cross-sectional design (diameters, perimeters, cortical thickness, CSMI, buckling ratio) or bone strength (BSIs, SSI). Bone trabecular structure can be assessed quasi-histomorphometrically by HR-pQCT. However, in this case the biomechanical interpretation of the data may be limited because the methodology does not capture the directional disposition of the trabecular network in relation to the direction of the forces which would break the bone. Muscle force can be easily (though indirectly) evaluated as the muscle cross-sectional area, which can be deprived of its fat content by filtration. Of course, dynamometrical data of the real muscle force are more suitable for this kind of analysis.

Image-derived muscle strength indicators usually correlate positively with all the above bone mass or strength indicators or with the CSMI. Typically, in normal individuals, bone mass (tibial + fibula BMC in pQCT scans) correlates linearly with the maximal muscle CSA of the calf, comprising the origin (Fig. 6a). Figure 6b shows the relationship between the A-P bending CSMI of the tibia and calf muscle CSA in the same cohort.

In agreement with the mechanostat theory, these correlations can evaluate the efficiency of the servo-controlled adaptation of bone design as a function of mechanical usage, and also distinguish between “mechanical” and “systemic” osteopenias as previously described. These relationships tend to differ greatly between men and women, chiefly because of (1) the larger values of all “extensive” indicators usually observed in male individuals, as a result of androgen-influences on both muscles and bones, with their obvious mechanical consequences, and (2) the estrogen-induced accumulation of bone mass (mostly trabecular tissue) per unit of muscle mass observed in premenopausal females, which tend to disappear after menopause. On the other hand, correlations of muscle indicators with the bone stiffness indicator, cortical vBMD, or other geometric indicators as the endocortical perimeter, cortical thickness, or the buckling ratio (ie,

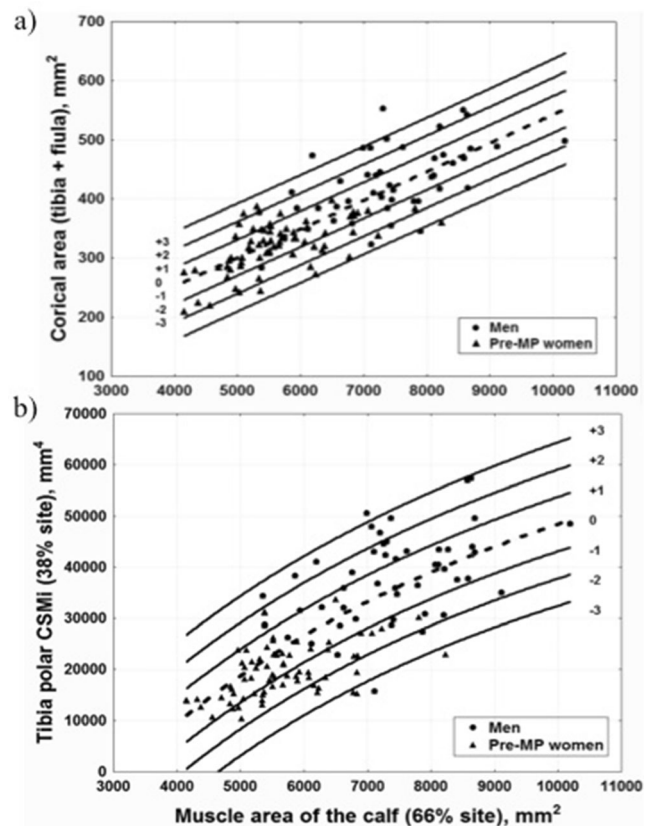


Fig. 6 (a) Relationships between the maximal cross-sectional muscle area of the calf (x) and (a) the cortical bone area of tibia + fibula (y); (b) polar CSMI of the tibia cross-sectional cortical bone area (y), both scanned by pQCT at 66 % of the tibia height in a representative sample of healthy men and premenopausal women. The Z-scores of the corresponding distributions are indicated as a reference

variables which are not supposed to be directly regulated by bone mechanostat) are rather weak.

Imaging Muscle/Bone Force/Stress (Mechanical, Dynamic) Relationships. (Combined dynamometric + Cross-Sectional Methodologies) → Safety Factors Estimation → True Diagnosis of Bone Fragility

Stress (σ) is defined as a force divided by the transversal area on which it actuates. The maximal effective compression force, *usual* F_{max} induced by a contraction of the regional muscles on a long bone, which can be assumed to resist mostly uniaxial compression can be measured dynamometrically. In normal conditions, *usual* σ_{max} is about 30 N / mm². It was estimated from experimental measurements that, also in normal conditions, the maximal stress a bone can resist in compression prior to fracture is $F_x \sigma_{max} = 180$ N / mm². Thus, and according to the Utah Paradigm of Skeletal Physiology [52], this would give a “safety factor” $SF = F_x \sigma_{max} / \text{usual } \sigma_{max} =$ about 6 to normal bones working in compression. This permits calculation of the theoretically *necessary* cortical bone CSA_t required to support $F_x \sigma_{max}$ in

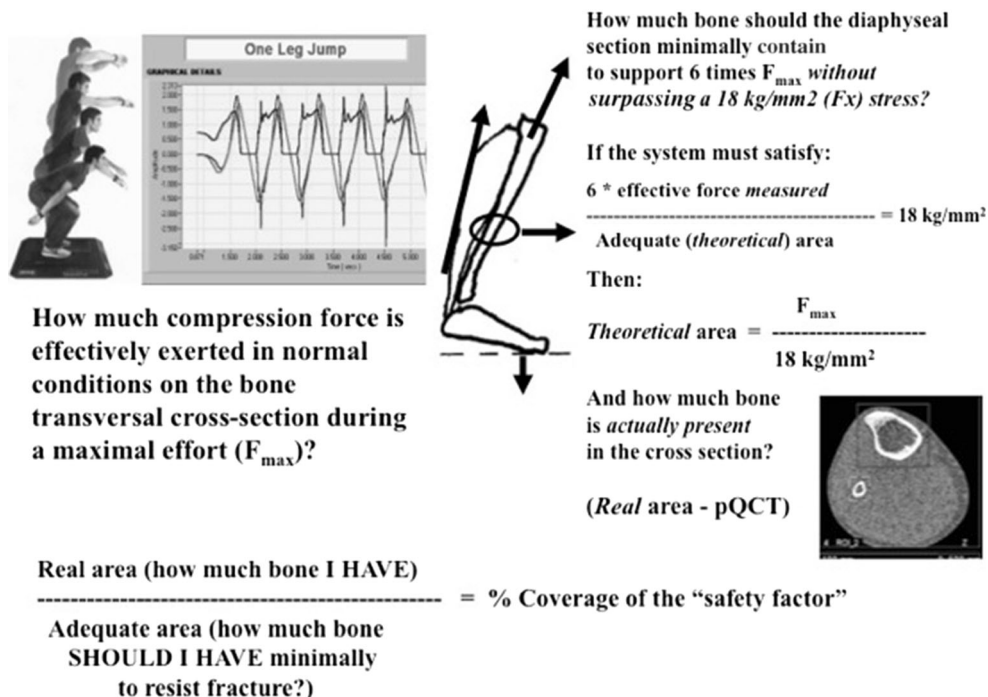
practical terms as $CSA_t = 6 * usual F_{max} (kg) / 18 \text{ kg/mm}^2$, expressed in mm^2 . As long as the real bone CSA of the individual studied (CSA_r) can be directly determined by pQCT or similar techniques in the same area units, the percent-relationship, $100 * CSA_r / CSA_t$ should estimate in what proportion the bone satisfies the SF predicted by the paradigm at the studied region and concerning the applied mode of deformation. This procedure is schematized in Fig. 7 for a situation in which the distal tibia was selected for study as a bone region known to resist mostly uniaxial stress during customary mechanical usage [53•, 54]. Whilst such approaches are only applicable in this manner to cortical bone (which varies little in density in adulthood outside of pathologic conditions and old age), there also exists a relationship between trabecular bone compressive strength and its apparent density [55]. More precisely, the relationship is well described by power functions with exponents that are somewhat depending on the anatomic site. However, assuming an exponent of 2 seems to be a reasonable general approach [56]. Hence, this idea could likely be adapted for epiphyseal bone. This or similar approaches (after the necessary validation and standardization) could evaluate the degree of fragility for a given bone, in biophysically reliable (stress) units. Such evaluation, performed in an osteopenic individual, can estimate to what extent his/her osteopenia has impacted bone strength in the studied region, with the corresponding specificity concerning site and mode of deformation. Thus, this should be a more reliable method to diagnose *osteoporosis* than the mechanically-irrelevant, -2.5 DMO T-score limit established for standard DXA determinations.

Site-Specific Approaches

Imaging of the muscle-bone relationship has been used to provide information on both bone physiology in basic science, and pathophysiology within research and clinical settings. Muscle-bone strength indices (MBSIs) have been established previously [57]. Compressive MBSI is based on the relationship between muscle CSA (as a surrogate for maximal force) and bone CSA as a surrogate for bone mass—given the lack of significant variation in density of health cortical bone—which indicates bone’s compressive strength. Similarly, bending MBSIs were calculated as the relationship between muscle bending moment (the product of muscle CSA and tibia length) and axial moment of resistance indicating bone strength in bending. Compressive MBSIs in the tibia vary throughout the limb length [57], suggesting that the influence of body mass on bone geometry is not pronounced. However, when considering bones adapted to the same compressive strength by controlling for bone mass, longer bones (ie, those with a longer lever arm for bending moments) were stronger in antero-posterior bending than short bones. Similar results have subsequently been found in the upper limbs, with the addition of much stronger relationships between wider bones (ie, where the moment arm for torsional moments is greater) and strength in torsion when compressive strength was controlled for [58•]. This suggests that antero-posterior moments may be the dominating influence on lower limb bones, whereas in the upper limbs torsional moments are most important.

The influence of factors such as exercise participation or disuse conditions, age, gender, and pubertal stage on muscle-

Fig. 7 Calculation of bone safety factor (SF)



bone relationships have been considered. Examining the relationship between muscle and bone in exercise or disuse intervention studies is problematic. First, rates of adaptation in muscle strength, size, and bone strength are discordant, particularly in exercise - significant changes in muscle size can be seen within 3 weeks of resistance training [59], whereas mechanoadaptation of bone has time-constants around 1–2 years [60]. Existing interventional exercise studies have reported only very meagre increases in bone strength [61], hence, correlations between muscle and bone increases in these studies would likely be significantly weakened due to the compounding of large measurement errors relative to the absolute change in values. This could also explain the weak muscle-bone size side difference relationships found in studies of youth tennis players [62] and footballers.

In other studies of youth and elite tennis players [58, 63] whilst strong correlations between upper limb muscle and bone CSA were found ($R^2=0.73-0.86$) different muscle-bone relationships were found in the racquet and nonracquet arm, with bone:muscle ratio being greater in the racquet arm. The authors suggested that this may be a result of the influence of individual muscles on bone, or that the high-impact nature of tennis strokes requires the muscles to act in a very different way to habitual usage. Similarly, a study of derived muscle-bone indices in female controls and elite volleyball players found lower muscle-bone relationships in the athletes [57]. Conversely, in disuse studies the time course of detecting early bone and muscle loss is similar [64, 65], but muscle size changes are more pronounced [66]. No long-term (>1 year) controlled disuse intervention studies have been performed—however, muscle-bone relationships in spinal cord injury patients and controls were similar [67].

Another area of investigation is the effects of age and gender on muscle-bone relationships. Muscle-bone size indices have been shown to vary between genders and pubertal status in adolescents in both pQCT [68, 69] and DXA studies [70], with pubertal effects likely a result (at least in part) of the discordant timing of height velocity and lean mass and bone mass velocity during the pubertal growth spurt [71]. Gender effects have been proposed to be a result of additional bone mass accrued in women during childbearing years (potentially as a reservoir for calcium during fetal growth). Supporting this, effects of menopause on muscle-bone relationships have been found with women of child-bearing age having greater bone-muscle mass ratios [72]. Similarly, analysis of a DXA-based large cohort study found that whilst premenopausal women had a greater bone-muscle size ratio than postmenopausal women and men, the curves of the logarithmic equations for the relationships ran parallel to each other for all groups [31]. This is supportive of a common mechanical muscular influence on bone, with additional bone mass accrued during the childbearing years independent of muscular influence. Further to this, it has been suggested that extra bone

mass in women is not stored in accordance with the mechanical ‘need’ of bone regions—this is supported by contrasting findings with regard to gender differences in pQCT-derived muscle-bone size indices at weight-bearing and non-weight-bearing sites [57, 63]. However, when individuals within the same age and gender groups are considered, relationships between muscle and bone structure appear to be very consistent. For example, muscle-bone size ratios are similar within normal weight and overweight children [73], and even in the extreme disuse case of spinal cord injury patients [67]. Alongside the extreme exercise case of elite athletes, only in long-term anorexia nervosa patients are muscle-bone relationships found to differ from sedentary controls, with ratios decreasing with disease progression [74].

Within the clinical setting, muscle-bone ratios obtained from imaging have been proposed as a method to distinguish between primary and secondary bone disorders (Fig. 8). Primary bone disorders or ‘systemic osteopenias’ can be attributed to dysfunction in bone metabolism/adaptation—hence, whilst muscle mass is normal bone mass is lower than expected. Conversely, secondary bone defects or ‘disuse osteopenias’ are where the bone’s adaptive processes appear to function correctly but the low bone mass is secondary to so-called sarcopenia or dynapenia. Finally, mixed bone defects occur when muscle mass is low, and bone-muscle ratio is lower than expected—indicating dysfunction in bone adaptation in addition to a lower muscle stimulus to the bone. Indeed, a similar schema was employed in analysis of pQCT-derived muscle-bone ratios. The schema could discriminate between healthy children and primary bone defects in frequent fracture patients and kidney transplant patients, and secondary bone defects in chronic renal failure patients [69]. DXA-derived indices of lean body mass and bone mass also showed children with osteogenesis imperfecta to have a primary bone

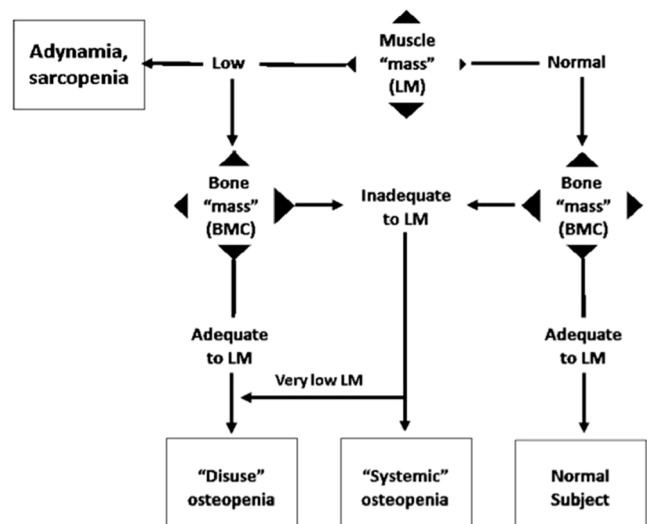


Fig. 8 Didactic representation of the 3 different etiologies proposed for all bone-weakening diseases, as referred to in the text

defect, and frequent fracture patients and those with spinal muscular atrophy to have a secondary bone defect [75].

This categorization of bone disorders has implications for patient treatment—*eg.* in secondary disorders, exercise may function as a treatment route, whereas primary disorders may necessitate a nutritional or pharmacologic intervention. Similarly study of muscle-bone relationships showed postmenopausal women with low muscle mass and high muscle-bone ratio having a very high risk of osteoporotic fracture [37]. A recent paper also proposed MRI-derived muscle-bone volume ratios in the thigh as an index of sarcopenia [76]. However, in order for these assessment methods to transfer fully into a clinical setting (*ie.* to be established as a typical tool in the clinician's arsenal), some standard methodology is required. Also, in the same way that osteopenia and osteoporosis have standardized definitions, a range of normative muscle-bone ratios can be established from large current datasets such in adults [77] and children [69, 75].

Conclusions

In conclusion, it appears that even 'crude' measurements of muscle and bone size can be used in classification of bone disorders and that more complex MBSIs have provided useful information pertaining primarily to bone mechanoadaptation and the influence of muscular action on bone. However, current imaging-based methods are likely limited in their ability to describe muscular influence—new methods such as 3D ultrasound of muscle may help future studies better approximate the muscle-bone relationship, both in research and clinical application.

Compliance with Ethics Guidelines

Conflict of Interest A. Ireland, J. Rittweger, and J. L. Ferretti all declare that they have no conflicts of interest.

Human and Animal Rights and Informed Consent This article does not contain any studies with human or animal subjects performed by any of the authors.

References

Papers of particular interest, published recently, have been highlighted as:

- Of importance

- Rittweger J, Ferretti JL. Imaging muscle-bone relationships—how to see the invisible. *Clion Rev Bone Min Metab*. 2014 [In press].
- Huxley AF, Simmons RM. Proposed mechanism of force generation in striated muscle. *Nature*. 1971;233:533–8.
- Jones D, Round J, de Haan A. *Skeletal muscle from molecules to movement*. London: Churchill Livingstone; 2004.
- Haxton HA. Absolute muscle force in the ankle flexors of man. *J Physiol*. 1944;103:267–73.
- Galban CJ, Maderwald S, Uffmann K, de Greiff A, Ladd ME. Diffusive sensitivity to muscle architecture: a magnetic resonance diffusion tensor imaging study of the human calf. *Eur J Appl Physiol*. 2004;93:253–62.
- Carter DR, Hayes WC. The compressive behavior of bone as a two-phase porous structure. *J Bone Joint Surg Am*. 1977;59:954–62.
- Schaffler MB, Burr DB. Stiffness of compact bone: effects of porosity and density. *J Biomech*. 1988;21:13–6.
- Alho A, Husby T, Hoiseith A. Bone mineral content and mechanical strength. An *ex vivo* study on human femora at autopsy. *Clin Orthop Relat Res*. 1988;227:292–7.
- Jämsä T, Jalovaara P, Peng Z, Väänänen HK, Tuukkanen J. Comparison of three-point bending test and peripheral quantitative computed tomography analysis in the evaluation of the strength of mouse femur and tibia. *Bone*. 1998;23:155–61.
- Ferretti JL, Capozza RF, Zanchetta JR. Mechanical validation of a tomographic (pQCT) index for noninvasive estimation of rat femur bending strength. *Bone*. 1996;18:97.
- Wilhelm G, Felsenberg D, Bogusch G, Willnecker J, Thaten J, Gummert P. Biomechanical examinations for validation of the bone strength strain index SSI, calculated by peripheral quantitative computer tomography. In: Lyritis G, editor. *Musculoskeletal interactions*. Athens: Hylonome; 1999. p. 105–8.
- Capozza RF, Rittweger J, Reina PS, Mortarino P, Nociolino LM, Feldman S, et al. pQCT-assessed relationships between diaphyseal design and cortical bone mass and density in the tibiae of healthy sedentary and trained men and women. *J Musculoskelet Neuronal Interact*. 2013;13:195–205. *Analyses of tibial diaphyseal design, proposing bone strength indices, which indicate the efficiency of bone mechanoadaptation in distributing cortical bone mass*.
- Burr DB. Muscle strength, bone mass, and age-related bone loss. *J Bone Miner Res*. 1997;12:1547–51.
- Arden NK, Spector TD. Genetic influences on muscle strength, lean body mass, and bone mineral density: a twin study. *J Bone Miner Res*. 1997;12:2076–81.
- Chen Z, Lohman TG, Stini WA, Ritenbaugh C, Aickin M. Fat or lean tissue mass: which one is the major determinant of bone mineral mass in healthy postmenopausal women? *J Bone Miner Res*. 1997;12:144–51.
- Nguyen TV, Howard GM, Kelly PJ, Eisman JA. Bone mass, lean mass, and fat mass: same genes or same environments? *Am J Epidemiol*. 1998;147:3–16.
- Ferretti JL, Capozza RF, Cointy GR, Capigliani R, Roldan EJ, Zanchetta JR. Densitometric and tomographic analyses of musculoskeletal interactions in humans. *J Musculoskelet Neuronal Interact*. 2000;1:31–4.
- Cointy GR, Capozza RF, Ferretti SE, et al. Absorptiometric assessment of muscle-bone relationships in humans: reference, validation, and application studies. *J Bone Miner Metab*. 2005;23(Suppl):109–14.
- Myburgh KH, Charette S, Zhou L, Steele CR, Arnaud S, Marcus R. Influence of recreational activity and muscle strength on ulnar bending stiffness in men. *Med Sci Sports Exerc*. 1993;25:592–6.
- Villa ML, Marcus R, Ramirez Delay R, Kelsey JL. Factors contributing to skeletal health of postmenopausal Mexican-American women. *J Bone Miner Res*. 1995;10:1233–42.
- Schoenau E, Neu CM, Rauch F, Manz F. The development of bone strength at the proximal radius during childhood and adolescence. *J Clin Endocrinol Metab*. 2001;86:613–8.
- LeBlanc A, Lin C, Shackelford L, et al. Muscle volume, MRI relaxation times (T₂), and body composition after spaceflight. *J Appl Physiol*. 2000;89:2158–64.

23. Gustavsson A, Thorsen K, Nordström P. A 3-year longitudinal study of the effect of physical activity on the accrual of bone mineral density in healthy adolescent males. *Calcif Tissue Int.* 2003;73:108–14.
24. Rico H, Revilla M, Villa LF, Ruiz-Contreras D, Hernández ER, Alvarez de Buergero M. The four-compartment models in body composition: data from a study with dual-energy X-ray absorptiometry and near-infrared interactance on 815 normal subjects. *Metabolism.* 1994;43:417–22.
25. Compston JE, Bhambhani M, Laskey MA, Murphy S, Khaw KT. Body composition and bone mass in post-menopausal women. *Clin Endocrinol (Oxf).* 1992;37:426–31.
26. Tsunenari T, Tsutsumi M, Ohno K, Yamamoto Y, Kawakatsu M, Shimogaki K, et al. Age- and gender-related changes in body composition in Japanese subjects. *J Bone Miner Res.* 1993;8:397–402.
27. Khosla S, Atkinson EJ, Riggs BL, Melton LJ. Relationship between body composition and bone mass in women. *J Bone Miner Res.* 1996;11:857–63.
28. Valdimarsson O, Kristinsson JO, Stefansson SO, Valdimarsson S, Sigurdsson G. Lean mass and physical activity as predictors of bone mineral density in 16-20 year old women. *J Intern Med.* 1999;245:489–96.
29. Ferretti JL, Schiessl H, Frost HM. On new opportunities for absorptiometry. *J Clin Densitom.* 1998;1:41–53.
30. Ferretti JL, Capozza RF, Cointy GR, García SL, Plotkin H, Alvarez Filgueira ML, et al. Gender-related differences in the relationship between densitometric values of whole-body bone mineral content and lean body mass in humans between 2 and 87 years of age. *Bone.* 1998;22:683–90.
31. Capozza RF, Cointy GR, Cure-Ramírez P, Ferretti JL, Cure-Cure C. A DXA study of muscle-bone relationships in the whole body and limbs of 2512 normal men and pre- and post-menopausal women. *Bone.* 2004;35:283–95.
32. Martin R, Burr D, Sharkley N. *Skeletal tissue mechanics.* New York: Springer; 1998.
33. Järvinen TL, Kannus P, Sievänen H. Estrogen and bone—a reproductive and locomotive perspective. *J Bone Miner Res.* 2003;18:1921–31.
34. Cure-Cure C, Capozza RF, Cointy GR, Meta M, Cure-Ramírez P, Ferretti JL. Reference charts for the relationships between dual-energy X-ray absorptiometry-assessed bone mineral content and lean mass in 3,063 healthy men and premenopausal and postmenopausal women. *Osteoporos Int.* 2005;16:2095–106.
35. Cointy GR, Capozza RF, Negri AL, Roldán EJ, Ferretti JL. Biomechanical background for a noninvasive assessment of bone strength and muscle-bone interactions. *J Musculoskelet Neuronal Interact.* 2004;4:1–11.
36. Ferretti JL, Cointy GR, Capozza RF, Frost HM. Bone mass, bone strength, muscle-bone interactions, osteopenias and osteoporoses. *Mech Ageing Dev.* 2003;124:269–79.
37. Capozza RF, Cure-Cure C, Cointy GR, Meta M, Cure P, Rittweger J, et al. Association between low lean body mass and osteoporotic fractures after menopause. *Menopause.* 2008;15:905–13.
38. Schneider P, Biko J, Reiners C, Demidchik Y, Drozd V, Capozza R, et al. Impact of parathyroid status and Ca and vitamin-D supplementation on bone mass and muscle-bone relationships in 208 Belarussian children after thyroidectomy because of thyroid carcinoma. *Exp Clin Endocrinol Diabetes.* 2004;112:444–50.
39. Cotofana S, Hudelmaier M, Wirth W, Himmer M, Ring-Dimitriou S, Sängler AM, et al. Correlation between single-slice muscle anatomic cross-sectional area and muscle volume in thigh extensors, flexors and adductors of perimenopausal women. *Eur J Appl Physiol.* 2010;110:91–7.
40. Maughan RJ, Watson JS, Weir J. Strength and cross-sectional area of human skeletal muscle. *J Physiol.* 1983;338:37–49.
41. Häkkinen K, Häkkinen A. Muscle cross-sectional area, force production and relaxation characteristics in women at different ages. *Eur J Appl Physiol Occup Physiol.* 1991;62:410–4.
42. Fukunaga T, Miyatani M, Tachi M, Kouzaki M, Kawakami Y, Kanehisa H. Muscle volume is a major determinant of joint torque in humans. *Acta Physiol Scand.* 2001;172:249–55.
43. Akagi R, Takai Y, Ohta M, Kanehisa H, Kawakami Y, Fukunaga T. Muscle volume compared with cross-sectional area is more appropriate for evaluating muscle strength in young and elderly individuals. *Age Ageing.* 2009;38:564–9.
44. D'Antona G, Pellegrino MA, Adami R, Rossi R, Carlizzi CN, Canepari M, et al. The effect of ageing and immobilization on structure and function of human skeletal muscle fibres. *J Physiol.* 2003;552:499–511.
45. Krivickas LS, Ansved T, Suh D, Frontera WR. Contractile properties of single muscle fibers in myotonic dystrophy. *Muscle Nerve.* 2000;23:529–37.
46. de Haan A, de Ruiter CJ, van Der Woude LH, Jongen PJ. Contractile properties and fatigue of quadriceps muscles in multiple sclerosis. *Muscle Nerve.* 2000;23:1534–41.
47. Neu CM, Rauch F, Rittweger J, Manz F, Schoenau E. Influence of puberty on muscle development at the forearm. *Am J Physiol Endocrinol Metab.* 2002;283:E103–7.
48. Morse CI, Tolfrey K, Thom JM, Vassilopoulos V, Maganaris CN, Narici MV. Gastrocnemius muscle specific force in boys and men. *J Appl Physiol.* 2008;104:469–74.
49. Herzog W, Sartorio A, Lafortuna CL, et al. Commentaries on viewpoint: can muscle size fully account for strength differences between children and adults? *J Appl Physiol.* 2011;110:1750–3. discussion 1754.
50. Delmonico MJ, Harris TB, Visser M, et al. Longitudinal study of muscle strength, quality, and adipose tissue infiltration. *Am J Clin Nutr.* 2009;90:1579–85.
51. Goodpaster BH, Carlson CL, Visser M, Kelley DE, Scherzinger A, Harris TB, et al. Attenuation of skeletal muscle and strength in the elderly: the Health ABC Study. *J Appl Physiol.* 2001;90:2157–65.
52. Frost H. *The Utah paradigm of skeletal physiology volume II.* Athens: ISMNI; 2004.
53. Capozza RF, Feldman S, Mortarino P, Reina PS, Schiessl H, Rittweger J, et al. Structural analysis of the human tibia by tomographic (pQCT) serial scans. *J Anat.* 2010;216:470–81. *Study showing that tibial bone structure through its length reflects adaptation to the loading regimes (eg, compression, bending, torsion) expected at the respective sites. Also, study proposes ratio of bone mass at 5% tibial length (primarily trabecular bone) to that at 15% length (primarily cortical bone) as a method of evaluating trabecular and cortical bone status at sites exposed to similar stress regimes.*
54. Feldman S, Capozza RF, Mortarino PA, Reina PS, Ferretti JL, Rittweger J, et al. Site and sex effects on tibia structure in distance runners and untrained people. *Med Sci Sports Exerc.* 2012;44:1580–8.
55. Ebbesen EN, Thomsen JS, Beck-Nielsen H, Nepper-Rasmussen HJ, Mosekilde L. Lumbar vertebral body compressive strength evaluated by dual-energy X-ray absorptiometry, quantitative computed tomography, and ashing. *Bone.* 1999;25:713–24.
56. Carter DR, Hayes WC. Bone compressive strength: the influence of density and strain rate. *Science.* 1976;194:1174–6.
57. Rittweger J, Beller G, Ehrig J, et al. Bone-muscle strength indices for the human lower leg. *Bone.* 2000;27:319–26.
58. Ireland A, Maden-Wilkinson T, McPhee J, Cooke K, Narici M, Degens H, et al. Upper limb muscle-bone asymmetries and bone adaptation in elite youth tennis players. *Med Sci Sports Exerc.* 2013;45:1749–58. *Shows the limitations of using local muscle CSA as a surrogate for muscular forces acting on the bone, and through analysis of MBSIs displays evidence of a dominating influence of torsional strains on humeral bone adaptation.*

59. Seynnes OR, de Boer M, Narici MV. Early skeletal muscle hypertrophy and architectural changes in response to high-intensity resistance training. *J Appl Physiol*. 2007;102:368–73.
60. Rittweger J, Felsenberg D. Recovery of muscle atrophy and bone loss from 90 days bed rest: results from a one-year follow-up. *Bone*. 2009;44:214–24.
61. Ireland A, Rittweger J, Degens H. The influence of muscular action on bone strength via exercise. *Clin Rev Bone Min Metab*. 2013;12:93–102.
62. Daly RM, Saxon L, Turner CH, Robling AG, Bass SL. The relationship between muscle size and bone geometry during growth and in response to exercise. *Bone*. 2004;34:281–7.
63. Ireland A, Maden-Wilkinson T, Ganse B, Degens H, Rittweger J. Effects of age and starting age upon side asymmetry in the arms of veteran tennis players: a cross-sectional study. *Osteoporos Int*. 2014;25:1389–400.
64. Rittweger J, Winwood K, Seynnes O, de Boer M, Wilks D, Lea R, et al. Bone loss from the human distal tibia epiphysis during 24 days of unilateral lower limb suspension. *J Physiol*. 2006;577:331–7.
65. de Boer MD, Maganaris CN, Seynnes OR, Rennie MJ, Narici MV. Time course of muscular, neural and tendinous adaptations to 23 day unilateral lower-limb suspension in young men. *J Physiol*. 2007;583:1079–91.
66. Rittweger J, Frost HM, Schiessl H, Ohshima H, Alkner B, Tesch P, et al. Muscle atrophy and bone loss after 90 days' bed rest and the effects of flywheel resistive exercise and pamidronate: results from the LTBR study. *Bone*. 2005;36:1019–29.
67. Bass SL, Eser P, Daly R. The effect of exercise and nutrition on the mechanostat. *J Musculoskelet Neuronal Interact*. 2005;5:239–54.
68. Macdonald HM, Kontulainen SA, Mackelvie-O'Brien KJ, Petit MA, Janssen P, Khan KM, et al. Maturity- and sex-related changes in tibial bone geometry, strength and bone-muscle strength indices during growth: a 20-month pQCT study. *Bone*. 2005;36:1003–11.
69. Schoenau E, Neu CM, Beck B, Manz F, Rauch F. Bone mineral content per muscle cross-sectional area as an index of the functional muscle-bone unit. *J Bone Miner Res*. 2002;17:1095–101.
70. Schiessl H, Frost HM, Jee WS. Estrogen and bone-muscle strength and mass relationships. *Bone*. 1998;22:1–6.
71. Rauch F, Bailey DA, Baxter-Jones A, Mirwald R, Faulkner R. The 'muscle-bone unit' during the pubertal growth spurt. *Bone*. 2004;34:771–5.
72. Ferretti JL, Capozza RF, Cointry GR, Garcia SL, Plotkin H, Alvarez Filgueira ML, et al. Gender-related differences in the relationship between densitometric values of whole-body bone mineral content and lean body mass in humans between 2 and 87 years of age. *Bone*. 1998;22:683.
73. Petit MA, Beck TJ, Shults J, Zemel BS, Foster BJ, Leonard MB. Proximal femur bone geometry is appropriately adapted to lean mass in overweight children and adolescents. *Bone*. 2005;36:568.
74. Bass SL, Saxon L, Corral AM, Rodda CP, Strauss BJ, Reidpath D, et al. Near normalisation of lumbar spine bone density in young women with osteopenia recovered from adolescent onset anorexia nervosa: a longitudinal study. *J Pediatr Endocrinol Metab*. 2005;18:897–907.
75. Crabtree NJ, Kibirige MS, Fordham JN, Banks LM, Muntoni F, Chinn D, et al. The relationship between lean body mass and bone mineral content in paediatric health and disease. *Bone*. 2004;35:965–72.
76. Maden-Wilkinson TM, McPhee JS, Rittweger J, Jones DA, Degens H. Thigh muscle volume in relation to age, sex and femur volume. *Age*. 2014;36:383–93.
77. Kelly TL, Wilson KE, Heymsfield SB. Dual energy X-Ray absorptiometry body composition reference values from NHANES. *PLoS One*. 2009;4:e7038.